

# Understanding the Land Use Dynamics and Environmental Impacts of Urbanization in Thimphu, Bhutan: A Satellite-Based Analysis

Indra Bahadur Chhetri

`indrachhetri.jnec@rub.edu.bt`

Royal University of Bhutan

Sangay Gyeltshen

Nagoya University

Kelzang Dema

Curtin University


---

## Research Article

**Keywords:** Google Earth Engine, land surface temperature, normalized difference vegetation index, land cover, MODIS.

**Posted Date:** March 15th, 2024

**DOI:** <https://doi.org/10.21203/rs.3.rs-3996182/v1>

**License:**   This work is licensed under a Creative Commons Attribution 4.0 International License. [Read Full License](#)

**Additional Declarations:** No competing interests reported.

---

# Abstract

The ability of the land surface temperature (LST) and normalized difference vegetation index (NDVI) to examine land surface change is regarded as an important climate variable. However, no significant systematic examination of urbanization concerning environmental variables has been undertaken in the narrow valley of Thimphu, Bhutan. Therefore, this study investigated the impact of land use and land cover (LULC) dynamics on LST, NDVI, and elevation; using Moderate Resolution Imaging Spectroradiometer (MODIS) data collected in Thimphu, Bhutan, from 2000 to 2020. The results showed that LSTs varied substantially among different land use types, with the highest occurring in built-up areas and the lowest occurring in forests. There was a strong negative linear correlation between the LST and NDVI in built-up areas, indicating the impact of anthropogenic activities. Moreover, elevation had a noticeable effect on the LST and NDVI, which exhibited very strong opposite patterns at lower elevations. In summary, LULC dynamics significantly influence LST and NDVI, highlighting the importance of understanding spatiotemporal patterns and their effects on ecological processes for effective land management and environmental conservation. Moreover, this study also demonstrated the applicability of relatively low-cost, moderate spatial resolution satellite imagery for examining the impact of urban development on the urban environment in Thimphu city.

## 1. Introduction

Urbanization and its impact on surrounding areas are fundamental aspects of developmental processes. The dynamic, multifunctional nature of urban environments necessitates a comprehensive understanding of landscape conditions and change patterns (Antrop, 2004; Robaa, 2011). Effective land planning, management, and development require accurate information on land use and land cover dynamics. Satellite imagery has emerged as a vital tool for studying spatiotemporal changes in land surface conditions, offering insights into the interactions between human activities and natural phenomena (Xiao & Weng, 2007; Yue et al., 2007).

The relationships between urbanization and environmental variables such as land surface temperature (LST) and normalized difference vegetation index (NDVI) have garnered significant attention in the literature (Otterman, 1974; Sagan et al., 1979). These indicators serve as crucial metrics for understanding land use/land cover characteristics and their interrelationships, with human actions increasingly driving changes in these variables over time. The distinct temporal profiles of the NDVI and LST allow for the identification of evolving land cover patterns, with varying land-use categories exhibiting significantly different mean LST and NDVI values (Yue et al., 2007).

Moreover, land use/land cover (LULC), surface albedo, and topographic elevation play pivotal roles in shaping the spatial distribution of LSTs (Deng et al., 2018a). The urban thermal environment, characterized by higher surface and air temperatures within urban areas than within rural surroundings, is a well-documented consequence of urbanization (Robaa, 2011). Thus, mapping changes in land use/land cover and analysing their relationships with environmental variables has become increasingly imperative.

While numerous studies have focused on measuring land-cover changes and understanding the causes of land-use change, limited research has explored the impact of these changes on local ecosystems, particularly concerning shifts in the LST and NDVI (Di Gregorio, 2005). Furthermore, existing studies have primarily concentrated on large urban centers, overlooking smaller cities such as Thimphu, and Bhutan, which possess unique geographical features and face distinct environmental challenges (Estoque et al., 2017; Kawashima, 1994). The scarcity of research on these smaller urban areas underscores the need for further exploration of their environmental dynamics.

Additionally, challenges related to data handling and accessibility hinder comprehensive analyses of land surface conditions, particularly in resource-constrained settings. However, the emergence of tools such as the Google Earth Engine (GEE) has facilitated the analysis of remote sensing data, offering opportunities for more efficient data processing (Ermida et al., 2020; Gorelick et al., 2017; Lambin et al., 2003).

In light of these considerations, this study aims to address several critical research questions. By leveraging Moderate Resolution Imaging Spectroradiometer (MODIS) data and the Google Earth Engine (GEE), we seek to fill the gap in understanding urban development dynamics in Thimphu city, Bhutan. Through a time-series cross-sectional study, we aimed to elucidate the relationship between urban LST and NDVI based on variations in land use/cover. By examining the impact of urban development on the urban environment over a substantial timeframe (2000 to 2022), our study endeavors to provide insights into the evolving landscape of Thimphu city and its environmental implications.

## 2. Materials and Methods

### 2.1 Experimental site

Thimphu city (Thromde) is located in the west-central part of Bhutan, with latitudes of 27°8' to 27°59', and longitudes of 89°13' to 89°46', a population of 114,551, and a total area of 26 km<sup>2</sup> (Figure 1). Thimphu's approximate altitude ranges from 2,240 to 2,648 m asl with the surrounding hills rising over 3800 m asl. The city part of the valley enjoys an alpine mountain climate with a warm summer and cold and dry winter with less rain in the monsoon season than in the east and south. The annual rainfall varies between 500 mm and 1000 mm. The average daily winter temperature varies between 5 and 15°C, and the average daily temperature during summer varies between 15 and 30°C. Thimphu city is accessible by road from India through the southern town of Phuentsholing, which is approximately 175 km away. It is also accessible by air from Paro, which is approximately 55 km long. Thimphu land use patterns specify the prevalence of negligible agricultural land (at almost 2%) in the lower eastern sectors, with forested land in the higher western areas and metropolitan borders. They are building clusters, clumps in traditional architecture on either end of the elongated city within the expanded Thimphu city boundary referred to in the Thimphu Structural Plan (TSP) as "urban villages".

### 2.2 Data collection

#### a. MODIS NDVI Data

The Terra Moderate Resolution Imaging Spectroradiometer (MODIS) was launched in December 1999 and offers a robust platform for monitoring various environmental parameters. The MODIS-derived MOD13Q1 V6.1 NDVI data product, comprising 16-day global composites at a spatial resolution of 250 meters, represents the atmospherically corrected bidirectional surface reflectance (BRDF), which is meticulously masked for water, clouds, heavy aerosols, and cloud shadows in the Geographic Lat/Long (WGS 84) projection. Understanding the characteristics of MODIS wavebands, vegetation indices, spatial resolutions (0.25 km, 0.50 km), and radiometric calibration techniques is imperative for leveraging readily available processed MODIS products to detect forest canopy changes at regional scales (Sruthi & Aslam, 2015). These data are readily accessible and can be seamlessly utilized within the Google Earth Engine (GEE) platform (KÜÇÜK MATCI et al., 2022). To assess the impact of land use/cover on NDVI, a key indicator of biomass and greenness, temporal variations in the NDVI were analysed. Specifically, the NDVI values for each image covering the years 2000 to 2020, with an interval of 5 years, were computed. This temporal analysis provides valuable insights into changing vegetation dynamics and the influence of land use/cover changes on ecosystem health and vitality.

#### b. MODIS LST Data

The MOD11A2 V6.1 LST data from MODIS, accessed through the Google Earth Engine (GEE) platform, have been pivotal for comprehensively evaluating the influence of land use/cover on land surface temperature (LST). These datasets, sourced from MODIS Land Surface Temperature and Emissivity (LST/E) products and provided by the United States Geological Survey (USGS), offer essential per-pixel temperature and emissivity information for understanding surface temperature dynamics. Specifically, the daily 1-kilometer LST product (MOD11A2), with a spatial resolution of 1 km and a temporal

resolution of 8 days, has provided valuable insights into the average values of clear-sky LSTs over 8 days. These level-3 MODIS global land surface temperature data, characterized by cloud-free spatial composites of gridded 16-day observations, have undergone meticulous radiometric correction and full calibration, rendering them suitable for use in scientific publications (Sona et al., 2012). The data accessed and processed through the GEE were integral to the analysis conducted in this study, enabling detailed investigations into land surface temperature variations and their relationships with land use/cover dynamics.

### c. Landuse/landcover data

The land use/cover maps procured from diverse sources were collected and scrutinized to ascertain land use/cover changes within the study area. Subsequently, an assessment was conducted to discern the impacts of these alterations on neighboring ecosystems, focusing particularly on changes in LST and NDVI. The origins of the diverse land use/cover maps employed, along with their respective characteristics, were documented and are presented in Table 1 for reference and comprehensive understanding.

Table 1: Land use/cover data characteristics for the study area

Year	Publication year	Source	Land-use type and its characteristics
LULC 2010	2011	(ICIMOD, 2011)	<p><b>Built-up:</b> Human-made structures; major road networks; large; examples: central business district (CBD), houses, dense villages/towns/cities, paved roads, asphalt, etc.</p> <p><b>Barren land:</b> Areas of rock or soil with very sparse to no vegetation for the entire year; examples: exposed rock or soil, mines, etc.</p>
LULC 2016	2015	(Rai & Phuentsho, 2016)	<p><b>Forest:</b> Typically, with a closed or dense canopy; examples: wooded dense vegetation, clusters of dense tall vegetation, etc.</p> <p><b>Vegetation:</b> Areas covered in homogeneous grasses with little to no taller vegetation; examples natural meadows, fields with sparse to no tree cover and pastures, etc.</p> <p><b>Agriculture land:</b> Emergent seasonal crops, rice paddies, and other heavily irrigated and inundated agriculture, etc.</p>
LULC 2020	2021	(Venter et al., 2022)	<p><b>Others (Water bodies, Snow, Clouds, etc.):</b> Areas where water was predominantly present throughout the year; for example, rivers, ponds lakes, etc.</p> <p><b>Snow:</b> Homogeneous areas of permanent snow or ice, typically only in mountain areas or highest latitudes; examples: glaciers, permanent snowpack, snow fields, etc.</p>

However, for the years 2000 and 2005, supervised classification techniques employing the maximum likelihood classifier classification procedure were applied in this study to classify the region into at least five major land use classes (consistent with other years).

### d. Elevation data

The investigation employed a Shuttle Radar Topography Mission (SRTM) digital elevation model (DEM) sourced from the United States Geological Survey (USGS; <https://www.usgs.gov/>), which is characterized by a spatial resolution of 30 meters. This SRTM DEM is noted for its vertical accuracy, expressed as linear error 90 (LE90), which falls within the range of 5-9 meters, with values not exceeding 16 meters, and a root mean square error (RMSE) of 9.73 meters, as documented by Mukul et al., (2017).

### 3. Methodology

The methodology encompasses several sequential steps, including image processing and classification, retrieval of NDVI, LST, spatiotemporal analysis for LST, NDVI, and Land Use/Land Cover (LULC), and intercorrelation among others (see Fig. 2).

#### 3.1 Landuse/landcover classification

Initially, to discern the spatial-temporal dynamics of land use/cover alterations, land use/cover maps spanning the years 2000, 2005, 2010, 2015, and 2020 were generated. Landsat 8 OLI Level 2 (see Table 2) was used for the classification of land use maps for the years 2000 and 2005. The analysis focused on five distinct land use/cover categories: forest, agriculture, urban/built-up, barren land, and others (encompassing waterbodies, glaciers, snow, clouds, etc.). The sources and attributes of these land use/cover maps are delineated in Table 1 and Table 2. However, for the years 2000 and 2005, supervised classification techniques employing the maximum likelihood classifier classification procedure were employed to categorize the region into no fewer than five primary land use classes for each temporal snapshot. Rigorous quantitative assessments were conducted to gauge the producer's and user's accuracy, overall accuracy, and kappa statistics. Through a stratified random sampling approach, a minimum of 100 testing samples (in pixels) were deployed for each class (Heydari & Mountrakis, 2018). The findings revealed significant accuracy, with an overall accuracy surpassing 86.67% and overall kappa statistics exceeding 0.70 across all classes.

Table 2  
Source of Landsat imagery and other characteristics

Year	Characteristics	Date of acquisition	Sources
2000	Atmospherically corrected Landsat 8 Surface Reflectance (SR)- USGS Landsat 8 Level 2, Collection 2, Tier 1 (LANDSAT/LC08/C02/T1_L2)	27th December, 2000	Imported through image collection in the GEE platform
2005	Spatial resolution: 30 m	7th November, 2005	

#### 3.2 Retrieval of the NDVI

Second, the NDVI was computed according to Eq. (1), which expresses the ratio of measured reflectance in the red (R) and near-infrared (NIR) spectral regions of the images. The formulation of this vegetation index typically involves different combinations of red and infrared bands, as green vegetation tends to absorb a significant portion of the spectrum in the red region and reflects more light in the infrared region than in built-up areas.

$$NDVI = \frac{NIR - RED}{NIR + RED}$$

1

Higher NDVI values are indicative of healthier vegetation cover, with the index ranging from - 1.0 to 1.0. Green plants tend to reflect more light in the near-infrared spectrum than in the visible range. Conversely, clouds, water, and snow exhibit greater reflectance in the visible spectrum than in the near-infrared spectrum, while the distinction between rock and bare soil is minimal (Jabal et al., 2022). Consequently, NDVI values for vegetation typically range from 0.1 to 0.75, with higher values correlating with denser plant canopies and increased greenness (Sobrino & Raissouni, 2000). Near-zero NDVI values are characteristic of the surrounding earth and rocks, whereas negative values are associated with water bodies such as rivers and dams (Tucker et al., 1986; Xiao & Weng, 2007).

#### 3.3 Retrieval of the LST

The LST of the study area for each image corresponding to 2000, 2005, 2010, 2015, and 2020 was computed utilizing MOD11A2 V6.1 LST data from MODIS (Pandey et al., 2022; Román et al., 2024). This dataset provides LST values expressed in Kelvin. The conversion of the digital numbers (DNs) of the LST data to degrees Celsius was achieved using Eq. (2) as follows:

$$\text{LST} = (\text{DN} * 0.02) - 273.15 \text{ } ^\circ \text{C}$$

2

Fourth, time-series cross-sectional studies were performed for each image for respective years. The pixel values of the LST and NDVI are generated based on each land use/cover type to reveal the variations in the LST and NDVI via different land surface characteristics and their different spatial patterns. Furthermore, the thermal environment and green space signatures of each land-use/cover type were examined to better understand the relationships between LST and land use/cover and, consequently, vegetation abundance indicators (NDVIs). All the data were subsampled to the study area and resampled to a spatial resolution of 30 m using the nearest neighbour algorithm in ESRI ArcGIS to match datasets for the NDVI, LST, and elevation analysis.

## 4. Results

### 4.1 Validation of MODIS-derived LSTs

The LST estimates obtained through the Moderate Resolution Imaging Spectroradiometer (MODIS) exhibit a commendable level of performance. A comprehensive evaluation of the efficacy of MODIS-derived LSTs was conducted by juxtaposing monthly MODIS-derived LST data with corresponding monthly temperature records maintained by the National Center for Hydrology and Meteorology (NCHM). The NCHM serves as a pivotal institution for the generation and dissemination of weather, climate, cryosphere, and hydrological information and services in Bhutan. Figure 3 illustrates the comparative analysis between the monthly MODIS-derived LST and concurrent temperature data sourced from the NCHM for the calendar year 2015. The graphical representation shows a notable concurrence between the MODIS-derived LST and the average temperature observations from the NCHM, thereby confirming the utility of the MODIS-derived LST as a credible proxy for LST assessments within the analytical framework.

### 4.2 Land use landcover classification, transition, and assessment

The land use classification outcomes derived from the maximum likelihood classification methodology within the ERDAS Imagine platform were subjected to rigorous evaluation employing Kohen kappa statistics for the temporal intervals of 2000 and 2005. In the assessment for the year 2000, a Kohen kappa coefficient of 0.65 was observed, which is indicative of substantial concordance beyond chance in the classification scheme. Complementing this metric, an overall accuracy rate of 86.67% underscored the efficacy of the classification approach in discerning land use patterns within the studied area. Conversely, for the temporal snapshot of 2005, a notable enhancement in classification agreement was observed, as evidenced by an elevated Kohen kappa coefficient of 0.88. This augmented coefficient signifies a heightened level of concordance in land use classification, further validated by an increased overall accuracy rate of 92.5%. The classification schema encompassed diverse land use categories including built-up areas, agricultural lands, barren lands, forests, and miscellaneous land types.

The Thimphu Valley has undergone notable urban expansion, as evidenced by a net increase of 28.46 km<sup>2</sup> in built-up areas between 2000 and 2020. Initially measured at 8.04 km<sup>2</sup> in 2000, the urban footprint expanded to 36.50 km<sup>2</sup> by 2020, reflecting a growth rate of 353.98% (see Table 3). The surge in construction activity witnessed during the years 2015-2020 contrasts with a period of subdued growth between 2012 and 2014, attributed to the cessation of construction financing, resulting in a freeze on ongoing projects and a scarcity of loans. This measure was instituted by the central bank to stem the

outflow of Indian rupees from Bhutan during a currency crisis (Bajaj, 2014). Consequently, urban expansion in Thimphu remained relatively stagnant until 2015, after which a significant construction boom ensued, leading to a remarkable increase of 23.81 km<sup>2</sup> in urban areas, equating to a growth rate of 187.63% (see Table 3).

Table 3: Land use/cover statistics in the study area during 2000-2020.

Land Use category	Area (Sq.km)					Area (%)				
	2000	2005	2010	2015	2020	2000	2005	2010	2015	2020
Built-up	8.04	10.08	14.99	12.69	36.50	2.0%	2.5%	3.6%	3.1%	8.9%
Agriculture	24.29	24.98	31.18	10.91	0.75	5.9%	6.1%	7.6%	2.7%	0.2%
Forest	324.44	306.57	338.80	370.34	292.92	78.9%	74.6%	82.4%	90.1%	71.3%
Barren area	53.93	60.13	24.59	14.11	80.05	13.1%	14.6%	6.0%	3.4%	19.5%
Others	0.31	9.25	1.42	2.91	0.76	0.1%	2.3%	0.3%	0.7%	0.2%

Furthermore, this expansion predominantly occurred in the northern and southern directions and central areas, owing to the constrained topography of the Wang Chhu River valley, as depicted in Figures 5 and 6. Conversely, forest coverage exhibited a declining trend over the same period, declining from 324.44 km<sup>2</sup> in 2000 to 292.92 km<sup>2</sup> in 2020, representing a reduction of 10.76%. The increase in barren land observed between 2000 and 2020 may be attributed to forest degradation resulting from prolonged dry seasons associated with climate change. These findings align with national forest inventory reports, which indicate that 2.3% of Bhutan's land has already experienced desertification, with an additional 34.1% at risk of such degradation (FRMD, 2016). Additionally, forest clearing to accommodate urban growth exacerbates this phenomenon.

Similarly, agricultural land experienced a modest increase from 2000 to 2010, with growth rates of 5.90% and 7.60% respectively. However, this trend reversed sharply from 2015 to 2020, with agricultural land decreasing from 2.70% to 0.20%. These observations underscore the trade-off between rapid urban development and the depletion of forest and agricultural areas, indicative of a transition towards increased urbanization. Figure 4 shows the area changed in four classes by year. The result also confirmed that Thimphu city has its built-up areas increased during 2000-2020 with net growth of 28.5 km<sup>2</sup>.

### 4.3 Visual interpretation of LULC, LST, and NDVI contrast

To provide a nuanced qualitative description of the spatial pattern, this study meticulously examined the temporal dynamics of land use and land cover (LULC) changes within the study area. By employing a classification scheme comprising six general categories, this research delves into the evolving landscape over time. Figures 5 and 6 offer insightful visual representations elucidating the spatial distribution of LULC, urban thermal characteristics, and vegetation cover across multiple years. Analysis of Thimphu's thermal imagery revealed notable disparities in LST, with the urban core consistently exhibiting a higher LST than the suburban locales. This discrepancy can be attributed to the prevalence of impermeable construction materials such as metals, asphalt, and concrete in urban infrastructure and transportation networks, which contribute to the urban heat island effect.

Conversely, examination of the NDVI reveals an inverse relationship, with built-up areas manifesting lower NDVI values than verdant landscapes such as forests, croplands, and parks. The visual depiction also underscores a declining trend in the NDVI values, which is indicative of the gradual encroachment of urbanization on vegetated areas. Moreover, beyond the urban core, regions characterized by snow, glaciers, and water bodies—classified as 'others' in LULC—exhibit distinct thermal and vegetative dynamics, with lower NDVI and LST values. This observation underscores the heterogeneity of land cover types and their corresponding thermal profiles within the study area, offering valuable insights into the complex interplay between urban development, vegetation cover, and thermal dynamics.

## 4.4 Relationships among the LST, NDVI, and elevation.

The spatial distribution analysis of LST and elevation revealed an inverse relationship, wherein the LST exhibited a gradual decrease with increasing elevation. This phenomenon is indicative of a discernible vertical variation rule, particularly within regions characterized by significant elevation differences. Geomorphologically, the study area features alternating terrains of valleys and hills, which further accentuate the observed vertical variation in the LST.

Remarkably, an examination of the elevation-dependent patterns of the NDVI from 2000 to 2020 also revealed a notable declining trend as elevation decreased (see Figures 7a & 7b). This phenomenon is presumed to be influenced by changes in climate drivers, including air temperature and precipitation, across varying elevation gradients, along with anthropogenic activities across the valley.

Furthermore, low-lying valleys within the study area typically coincide with areas of concentrated urban development. Here, the LST and NDVI demonstrated contrasting spatial distributions, with the LST exhibiting higher values in low valleys, while the NDVI exhibited lower values in areas with concentrated urban. These microlevel observations underscore the intricate relationship between land surface characteristics and urbanization dynamics.

To quantify these relationships, Figures 8 and 9 present symmetric correlations (subject to the assumption of a linear relationship) between LST, NDVI, and elevation for different years. The analysis revealed a strong negative correlation between both the LST and NDVI with elevation in 2000, which gradually decreased over subsequent years. This trend is attributed to factors such as the increasing influence of rising air temperatures due to anthropogenic activities and a relative decline in surface vegetation quality from 2000 to 2020. The results demonstrate the extent to which the observed changes in LULC and elevation can be linked to the spatial and temporal patterns of the LST in the city.

## 4.5 Relationships between the LST and NDVI and land use type.

The relationship between temperature and the NDVI has garnered considerable attention in the academic literature. For instance, Weng (2003) extensively analysed the association between LST and the NDVI across various land use/cover categories. Utilizing seven distinct land use/cover types—commercial, industrial, residential, cropland, grassland, pasture, forest, and water—at multiple spatial scales, Weng observed a consistent and significant inverse correlation between the LST and NDVI.

Similarly, Sobrino and Raissouni (2000) explored land-cover dynamics in Morocco by leveraging the inverse relationship between the NDVI and radiant surface temperature measurements derived from multitemporal Advanced Very High-Resolution Radiometer (AVHRR) imagery.

Table 4 presents the results of the linear regression analyses between the LST and NDVI for the different land use/cover types within the study area. In this table, 'y' denotes the mean LST associated with each land use/cover type, while 'x' represents the mean NDVI corresponding to the respective land use/cover type. The table further provides descriptive statistics such as the maximum, minimum, mean, standard deviation, Pearson correlation coefficient ( $r$ ), and R-squared ( $R^2$ ) values for each land use/cover category spanning the years 2000 to 2020, with a temporal interval of five years.

Analysis of the data revealed notable temperature disparities among land use/cover types, particularly between urban or built-up areas and vegetated surfaces. The maximum LSTs of the urban areas ranged from 20.94°C to 22.57°C, indicating comparatively higher temperatures. Moreover, discernible differences were observed in the mean LSTs between built-up areas and forests, highlighting distinct thermal characteristics associated with different land use/cover types.

Regression analyses revealed a significant inverse correlation between the LST and NDVI, particularly in built-up areas, with correlation coefficients as high as 0.88, indicating a strong-to-very-strong negative relationship. Conversely, barren land



exhibited a negative correlation in the year 2000 but transitioned to a strong positive correlation with LST and NDVI in subsequent years, with correlation coefficients ranging up to 0.67. In contrast, the forest region exhibited weak-to-moderate correlations (with correlation coefficients ranging from 0.27 to 0.50) between the LST and NDVI, which is indicative of a less pronounced relationship between the forest region and the other land use/cover types. This finding indicates that the NDVI and LST are closely correlated in several LULC categories, especially in vegetated lands. Additionally, with several policies and legal frameworks introduced that are forest-related national acts and policies, the average NDVI value has remained relatively consistent across all LULC types, which might be an indication of policy impact.

Table 4: Linear regression and correlation coefficients for the relationship between LST and NDVI by land use/cover type.

Land use	Year	Linear Representation form	LST (degree)				NDVI				LST vs NDVI	
			Min	Max	Mean	$\sigma$	Min	Max	Mean	$\sigma$	r	R <sup>2</sup>
Built-up	2000	$y = -0.0196x + 0.8989$	18.47	22.57	20.66	1.29	0.40	0.56	0.49	0.04	-0.64	0.41
	2005	$y = -0.0385x + 1.2022$	12.50	21.09	18.04	2.15	0.34	0.72	0.51	0.09	-0.88	0.77
	2010	$y = -0.0235x + 0.9495$	14.32	21.34	18.49	1.82	0.36	0.62	0.52	0.06	-0.67	0.44
	2015	$y = -0.0314x + 1.0609$	11.43	20.94	17.53	2.68	0.35	0.70	0.51	0.10	-0.83	0.69
	2020	$y = -0.0263x + 0.998$	11.42	21.57	17.51	2.63	0.35	0.70	0.54	0.08	-0.84	0.71
Forest	2000	$y = 0.0136x + 0.3868$	7.87	23.89	13.87	3.39	0.16	0.73	0.57	0.11	0.49	0.21
	2005	$y = 0.0082x + 0.5383$	6.21	20.91	12.12	3.01	0.26	0.76	0.64	0.09	0.27	0.07
	2010	$y = 0.0108x + 0.4842$	6.50	20.37	11.98	2.94	0.28	0.78	0.61	0.10	0.33	0.11
	2015	$y = 0.0118x + 0.4685$	5.76	20.52	11.83	3.50	0.24	0.84	0.61	0.12	0.34	0.12
	2020	$y = 0.018x + 0.4053$	5.78	20.35	11.49	2.82	0.25	0.80	0.61	0.10	0.50	0.25
Barren land	2000	$y = -0.0135x + 0.8378$	12.01	22.78	19.81	2.31	0.15	0.68	0.57	0.05	-0.63	0.40
	2005	$y = 0.0192x + 0.2145$	6.60	20.91	13.24	4.88	0.17	0.72	0.47	0.15	0.63	0.40
	2010	$y = 0.0229x + 0.1726$	9.11	20.67	14.05	4.08	0.27	0.71	0.49	0.14	0.67	0.45
	2015	$y = 0.0124x + 0.2842$	7.31	21.01	14.54	5.39	0.26	0.65	0.46	0.11	0.61	0.37
	2020	$y = 0.0124x + 0.2842$	6.53	21.41	13.94	5.05	0.20	0.71	0.46	0.14	0.64	0.40
Agriculture	2000	$y = 0.0165x + 0.191$	12.42	23.82	20.59	2.13	0.41	0.71	0.55	0.05	-0.77	0.44
	2005	$y = -0.0295x + 1.0903$	11.94	21.00	18.01	2.30	0.40	0.72	0.56	0.07	-0.91	0.82
	2010	$y = -0.0231x + 0.9836$	11.54	21.25	18.06	2.44	0.40	0.72	0.57	0.07	-0.80	0.64
	2015	$y = -0.0289x + 1.0513$	11.43	20.94	17.50	2.36	0.35	0.71	0.55	0.09	-0.74	0.54
	2020	$y = 0.0198x + 0.124$	8.18	20.11	14.51	6.00	0.21	0.60	0.41	0.20	0.61	0.37

## 5. Discussion

Our study aligns seamlessly with previous research efforts, reinforcing and expanding upon established findings in the field. The unique topographical characteristics of Thimphu, Bhutan, which is situated within a mountainous region, necessitate a nuanced examination of the relationships between land use dynamics and environmental variables. By contextualizing our investigation within this distinctive geographical setting, we contribute to a growing body of literature that recognizes the importance of considering regional idiosyncrasies in understanding the environmental impacts of urbanization.

Building upon the foundational work of Deng et al.,(2018b); Sun et al., (2021); Maharjan et al., (2012), who emphasized the role of impervious surfaces in driving urban heat islands, our study corroborates the urban heat island effect within the specific context of Thimphu. This confirmation underscores the universality of this phenomenon across diverse urban landscapes, thereby enhancing the generalizability of research findings in urban climatology.

Additionally, our identification of a strong negative correlation between LST and NDVI in built-up and agricultural lands echoes the conclusions drawn by Gorgani et al., (2013); Sun et al., (2012), highlighting the pivotal role of vegetation in moderating surface temperatures in urban environments. By replicating this relationship in the mountainous terrain of Thimphu, our study underscores the resilience of ecological principles across varied landscapes, contributing to a deeper understanding of ecosystem dynamics in mountainous urban areas.

Moreover, our analysis of spatial distribution patterns along elevation gradients aligns with the observations made by Gorgani et al., (2013) regarding the influence of topography on microclimatic conditions. The consistent findings across disparate geographical settings underscore the robustness of the relationship between elevation and land surface variables, emphasizing the need for comprehensive assessments that account for topographical heterogeneity.

By documenting temporal changes in land use dynamics and corroborating prevailing trends identified in studies on urbanization and land cover change, our research underscores the continuity of landscape transformation processes over time. This alignment with past research not only validates the persistence of observed trends but also underscores the imperative of adopting sustainable land management practices to mitigate environmental degradation in rapidly urbanizing regions. Moreover, this study demonstrated similar findings to understand the extent to which the observed changes in LULC and elevation can be linked to the spatial and temporal patterns of the LST, as observed in Ilorin, Nigeria (Njoku & Tenenbaum, 2022).

In summary, our study's alignment with past research reflects a concerted effort to build upon existing knowledge frameworks and advance scientific understanding in the field of urban environmental studies. By embracing the interdisciplinary nature of urban climatology and integrating insights from diverse geographical contexts, our research contributes to a holistic understanding of the complex interplay between urbanization, land use dynamics, and environmental sustainability.

## 6. Conclusion

This study utilized MODIS LST and NDVI datasets to examine the spatial distribution patterns and interrelationships between the LST and NDVI in Thimphu, Bhutan. Further integration of land-use types and elevation facilitated a comprehensive analysis of these variables. This investigation explored the spatial distribution characteristics of the LST and NDVI, their quantitative relationships, and changes in the LST across various land-use types over the period from 2000 to 2020.

The key findings from the study are as follows:

- I. Significant differences in LST were observed among various land use types, with built-up areas exhibiting the highest LST of 22.57°C and forestland displaying the lowest LST of 5.76°C, showing an increasing trend over the study period.
- II. Strong negative linear correlations between LST and NDVI were observed for built-up and agricultural land, while other land-use types showed weak-to-weak positive linear correlations.

III. The opposite spatial distribution patterns of the NDVI and LST were noted along low-lying valleys.

IV. The study highlighted decreases in agricultural and forestland, accompanied by significant increases in urban/built-up and barren areas, with a temporary slowdown in urban growth observed during the years 2010-2015 due to the suspension of construction financing.

Additionally, fluctuations in vegetated areas, particularly in steeply sloping regions, were observed, with increases in barren land noted in transition zones between forests and built-up areas. Overall, this study underscores the utility of satellite remote sensing technology for monitoring landscape composition and its effects on vegetation indices at a regional scale. This study also provides evidence of the thermal impacts of impervious surfaces (e.g., built-up areas) compared to those of green spaces, emphasizing the importance of urban planning strategies that prioritize vegetation clustering and minimize impervious surfaces to create healthier and more comfortable urban environments. In summary, the findings offered valuable insights for urban planners and policymakers, highlighting the need to optimize urban landscape spatial patterns to enhance environmental quality and livability.

## Declarations

**Author Contributions:** Mr. Indra Bahadur Chhetri conceived the core idea of the research and wrote the manuscript. Mr. Sangay Gyeltshen and Mrs. Kelzang Dema analysed the spatial content and supported the writing of the manuscript. All the authors reviewed the manuscript and consented to the publication of this study.

**Funding details:** The author declares that no funding has been provided for this research.

**Conflict of interest:** The authors report that there are no competing interests to declare.

**Data Availability Declaration:** The authors confirm that the data supporting the findings of this study shall be provided with a reasonable request from the corresponding author.

## References

1. Antrop, M. (2004). Landscape change and the urbanization process in Europe. *Landscape and Urban Planning*, 67(1–4), 9–26. [https://doi.org/10.1016/S0169-2046\(03\)00026-4](https://doi.org/10.1016/S0169-2046(03)00026-4)
2. Bajaj, M. (2014). *Thimphu's Growing Pains-Challenges of Implementing the City Plan*.
3. Deng, Y., Wang, S., Bai, X., Tian, Y., Wu, L., Xiao, J., Chen, F., & Qian, Q. (2018a). Relationship among land surface temperature and LUCC, NDVI in typical karst area. *Scientific Reports*, 8(1), 1–12. <https://doi.org/10.1038/s41598-017-19088-x>
4. Deng, Y., Wang, S., Bai, X., Tian, Y., Wu, L., Xiao, J., Chen, F., & Qian, Q. (2018b). Relationship among land surface temperature and LUCC, NDVI in typical karst area. *Scientific Reports*, 8(1), 641. <https://doi.org/10.1038/s41598-017-19088-x>
5. Di Gregorio, A. (2005). *Land cover classification system: classification concepts and user manual: LCCS (Vol. 2)*. Food & Agriculture Org.
6. Ermida, S. L., Soares, P., Mantas, V., Göttsche, F. M., & Trigo, I. F. (2020). Google earth engine open-source code for land surface temperature estimation from the landsat series. *Remote Sensing*, 12(9), 1–21. <https://doi.org/10.3390/RS12091471>
7. Estoque, R. C., Murayama, Y., & Myint, S. W. (2017). Effects of landscape composition and pattern on land surface temperature: An urban heat island study in the megacities of Southeast Asia. *Science of the Total Environment*, 577, 349–359. <https://doi.org/10.1016/j.scitotenv.2016.10.195>
8. FRMD. (2016). *National Forest Inventory Report: Stocktaking Nation's Forest Resources Volume I: Vol. II*. <http://www.dofps.gov.bt/wp-content/uploads/2017/07/National-Forest-Inventory-Report-Vol1.pdf>

9. Gorelick, N., Hancher, M., Dixon, M., Ilyushchenko, S., Thau, D., & Moore, R. (2017). Google Earth Engine: Planetary-scale geospatial analysis for everyone. *Remote Sensing of Environment*, 202(2016), 18–27. <https://doi.org/10.1016/j.rse.2017.06.031>
10. Gorgani, S. A., Panahi, M., & Rezaie, F. (2013). *The Relationship between NDVI and LST in the urban area of Mashhad, Iran. November.*
11. Heydari, S. S., & Mountrakis, G. (2018). Effect of classifier selection, reference sample size, reference class distribution, and scene heterogeneity in per-pixel classification accuracy using 26 Landsat sites. *Remote Sensing of Environment*, 204(February 2017), 648–658. <https://doi.org/10.1016/j.rse.2017.09.035>
12. ICIMOD. (2011). *Land Cover of Bhutan 2020*. <https://doi.org/https://doi.org/10.26066/rds.8880>
13. Jabal, Z. K., Khayyun, T. S., & Alwan, I. A. (2022). Impact of Climate Change on Crops Productivity Using MODIS-NDVI Time Series. *Civil Engineering Journal (Iran)*, 8(6), 1136–1156. <https://doi.org/10.28991/CEJ-2022-08-06-04>
14. Kawashima, S. (1994). Relation between vegetation, surface temperature, and surface composition in the tokyo region during winter. *Remote Sensing of Environment*, 50(1), 52–60. [https://doi.org/10.1016/0034-4257\(94\)90094-9](https://doi.org/10.1016/0034-4257(94)90094-9)
15. KÜÇÜK MATCI, D., BAŞARAN, N., & AVDAN, U. (2022). Using multiple linear regression to analyze changes in forest area: the case study of Akdeniz Region. *International Journal of Engineering and Geosciences*, 7(3), 247–263. <https://doi.org/10.26833/ijeg.976418>
16. Lambin, E. F., Geist, H. J., & Lepers, E. (2003). Dynamics of Land-Use and Land-Cover Change in Tropical Regions. *Annual Review of Environment and Resources*, 28(1), 205–241. <https://doi.org/10.1146/annurev.energy.28.050302.105459>
17. Maharjan, M., Aryal, A., Man Shakya, B., Talchabhadel, R., Thapa, B. R., & Kumar, S. (2021). Evaluation of Urban Heat Island (UHI) Using Satellite Images in Densely Populated Cities of South Asia. *Earth*, 2(1), 86–110. <https://doi.org/10.3390/earth2010006>
18. Mukul, M., Srivastava, V., Jade, S., & Mukul, M. (2017). Uncertainties in the Shuttle Radar Topography Mission (SRTM) Heights: Insights from the Indian Himalaya and Peninsula. *Scientific Reports*, 7(December 2016), 1–10. <https://doi.org/10.1038/srep41672>
19. Njoku, E. A., & Tenenbaum, D. E. (2022). Quantitative assessment of the relationship between land use/land cover (LULC), topographic elevation and land surface temperature (LST) in Ilorin, Nigeria. *Remote Sensing Applications: Society and Environment*, 27, 100780.
20. Otterman, J. (1974). *Baring High-Albedo Soils by Overgrazing: A Hypothesized Desertification Mechanism.*
21. Pandey, P. C., Chauhan, A., & Maurya, N. K. (2022). Evaluation of earth observation datasets for LST trends over India and its implication in global warming. *Ecological Informatics*, 72, 101843. <https://doi.org/https://doi.org/10.1016/j.ecoinf.2022.101843>
22. Rai, A., & Phuentsho, P. (2016). *Land Use and Land Cover Assessment of Bhutan 2016 Technical Report.*
23. Robaa, S. M. (2011). Effect of urbanization and industrialization processes on outdoor thermal human comfort in Egypt. *International Journal of Meteorology*, 36(360), 111–125. <https://doi.org/10.4236/acs.2011.13012>
24. Román, M. O., Justice, C., Paynter, I., Boucher, P. B., Devadiga, S., Endsley, A., Erb, A., Friedl, M., Gao, H., Giglio, L., Gray, J. M., Hall, D., Hulley, G., Kimball, J., Knyazikhin, Y., Lyapustin, A., Myneni, R. B., Noojipady, P., Pu, J., ... Wolfe, R. (2024). Continuity between NASA MODIS Collection 6.1 and VIIRS Collection 2 land products. *Remote Sensing of Environment*, 302, 113963. <https://doi.org/https://doi.org/10.1016/j.rse.2023.113963>
25. Sagan, C., Toon, O. B., & Pollack, J. B. (1979). *Anthropogenic Albedo Changes and the Earth's Climate.* 206(4425), 1363–1368.
26. Sobrino, J. A., & Raissouni, N. (2000). Toward remote sensing methods for land cover dynamic monitoring: Application to Morocco. *International Journal of Remote Sensing*, 21(2), 353–366. <https://doi.org/10.1080/014311600210876>
27. Sona, N. T., Chen, C. F., Chen, C. R., Chang, L. Y., & Minh, V. Q. (2012). Monitoring agricultural drought in the lower mekong basin using MODIS NDVI and land surface temperature data. *International Journal of Applied Earth Observation and Geoinformation*, 18(1), 417–427. <https://doi.org/10.1016/j.jag.2012.03.014>

28. Sruthi, S., & Aslam, M. A. M. (2015). Agricultural Drought Analysis Using the NDVI and Land Surface Temperature Data; a Case Study of Raichur District. *Aquatic Procedia*, 4(lcwrcoe), 1258–1264. <https://doi.org/10.1016/j.aqpro.2015.02.164>
29. Sun, Q., Wu, Z., & Tan, J. (2012). The relationship between land surface temperature and land use/land cover in Guangzhou, China. *Environmental Earth Sciences*, 65(6), 1687–1694. <https://doi.org/10.1007/s12665-011-1145-2>
30. Tucker, C. J., Fung, I. Y., Keeling, C. D., & Gammon, R. H. (1986). Relationship between atmospheric CO2 variations and a satellite-derived vegetation index. *Nature*, 319(6050), 195–199. <https://doi.org/10.1038/319195a0>
31. Venter, Z. S., Barton, D. N., Chakraborty, T., Simensen, T., & Singh, G. (2022). Global 10 m Land Use Land Cover Datasets: A Comparison of Dynamic World, World Cover and Esri Land Cover. *Remote Sensing*, 14(16). <https://doi.org/10.3390/rs14164101>
32. Weng, Q. (2003). Fractal analysis of satellite-detected urban heat island effect. *Photogrammetric Engineering and Remote Sensing*, 69(5), 555–566. <https://doi.org/10.14358/PERS.69.5.555>
33. Xiao, H., & Weng, Q. (2007). The impact of land use and land cover changes on land surface temperature in a karst area of China. *Journal of Environmental Management*, 85(1), 245–257. <https://doi.org/10.1016/j.jenvman.2006.07.016>
34. Yue, W., Xu, J., Tan, W., & Xu, L. (2007). The relationship between land surface temperature and NDVI with remote sensing: Application to Shanghai Landsat 7 ETM+ data. *International Journal of Remote Sensing*, 28(15), 3205–3226. <https://doi.org/10.1080/01431160500306906>

## Figures

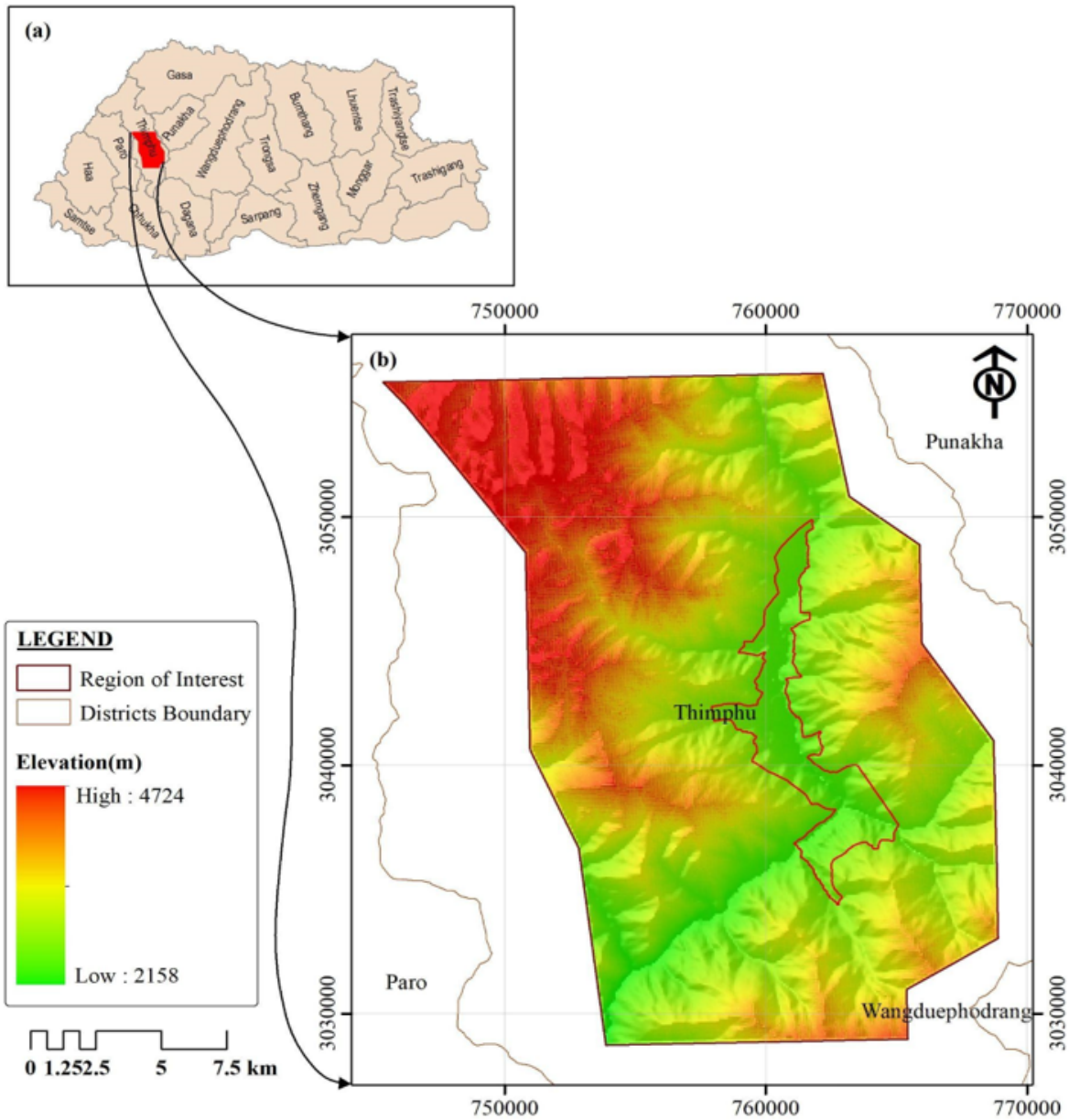


**Figure 1**

The geographical features of the study region: (a) the districts of Bhutan; (b) the study area including Thimphu city (region of interest)

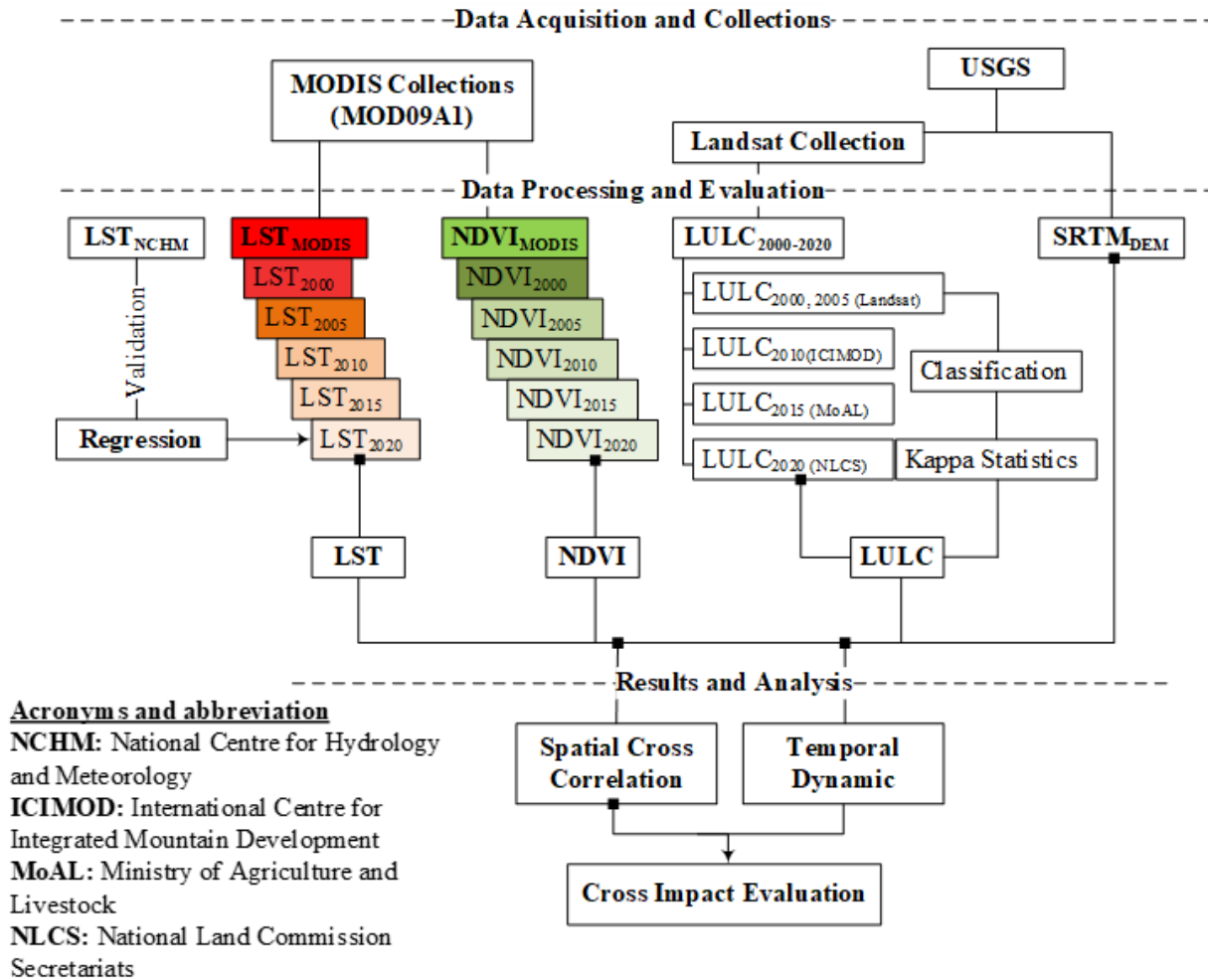
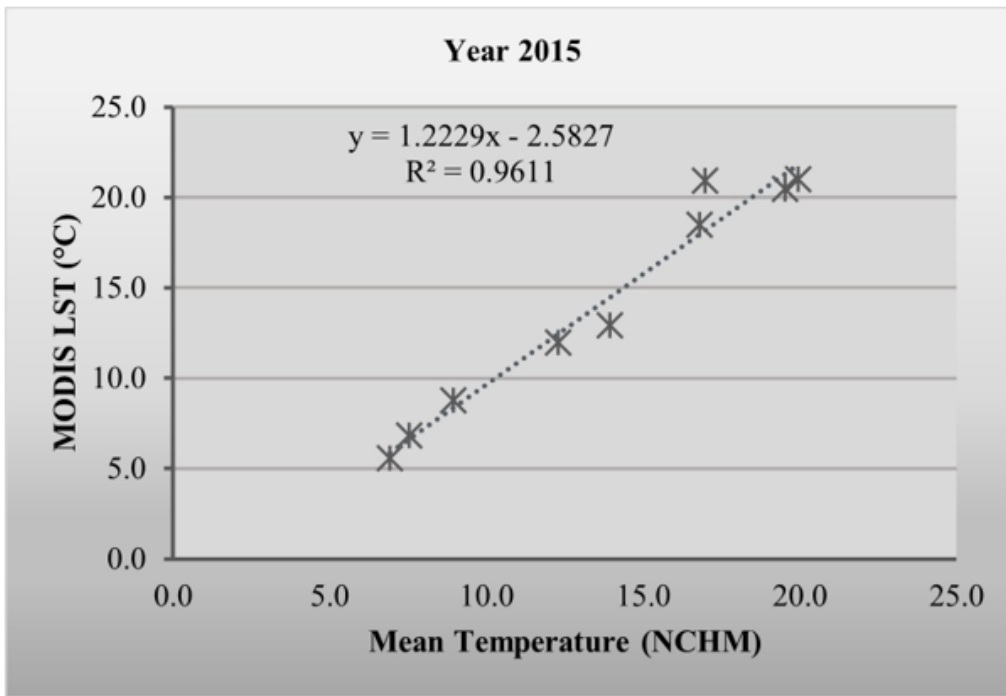


Figure 2

Framework for the general approach and methodology





**Figure 3**

Scatter plot showing the R-squared values obtained between the mean temperature from the NCHM and the MODIS-derived LST for 2015

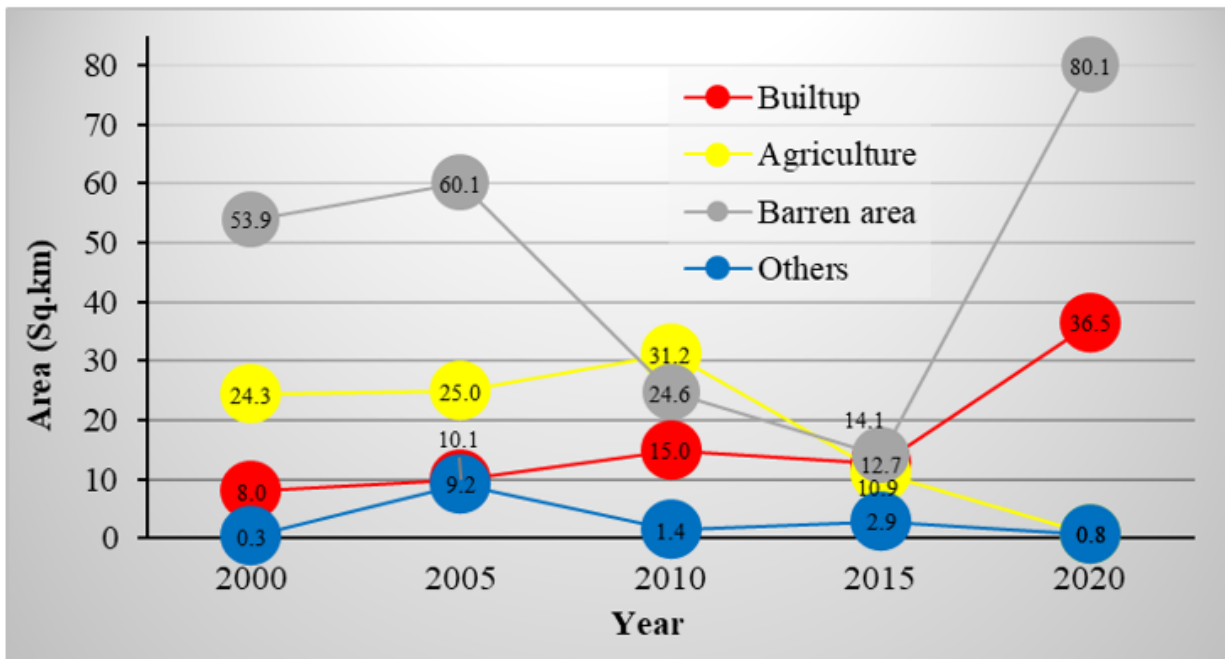


**Figure 4**

Temporal analysis of LULC in Thimphu city during the study period between 2000 and 2020. LULC (others) accounted for water bodies, snow, and glaciers.

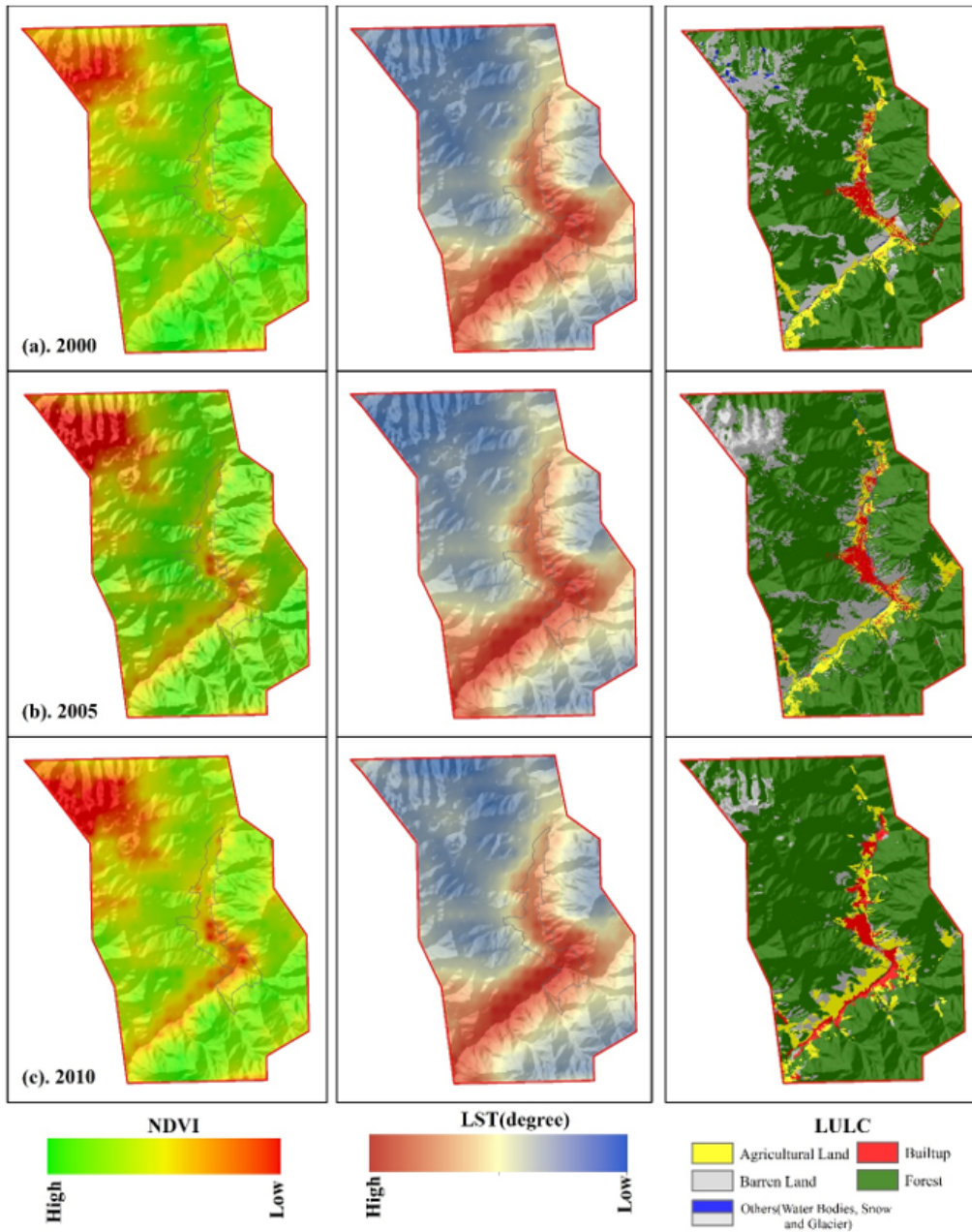


**Figure 5**

Spatial representation of the trends in the NDVI, LST, and LULC (a) NDVI, LST, and LULC images for the year 2000; (b) NDVI, LST, and LULC images for the year 2005; and (c) NDVI, LST and LULC images for the year 2010.

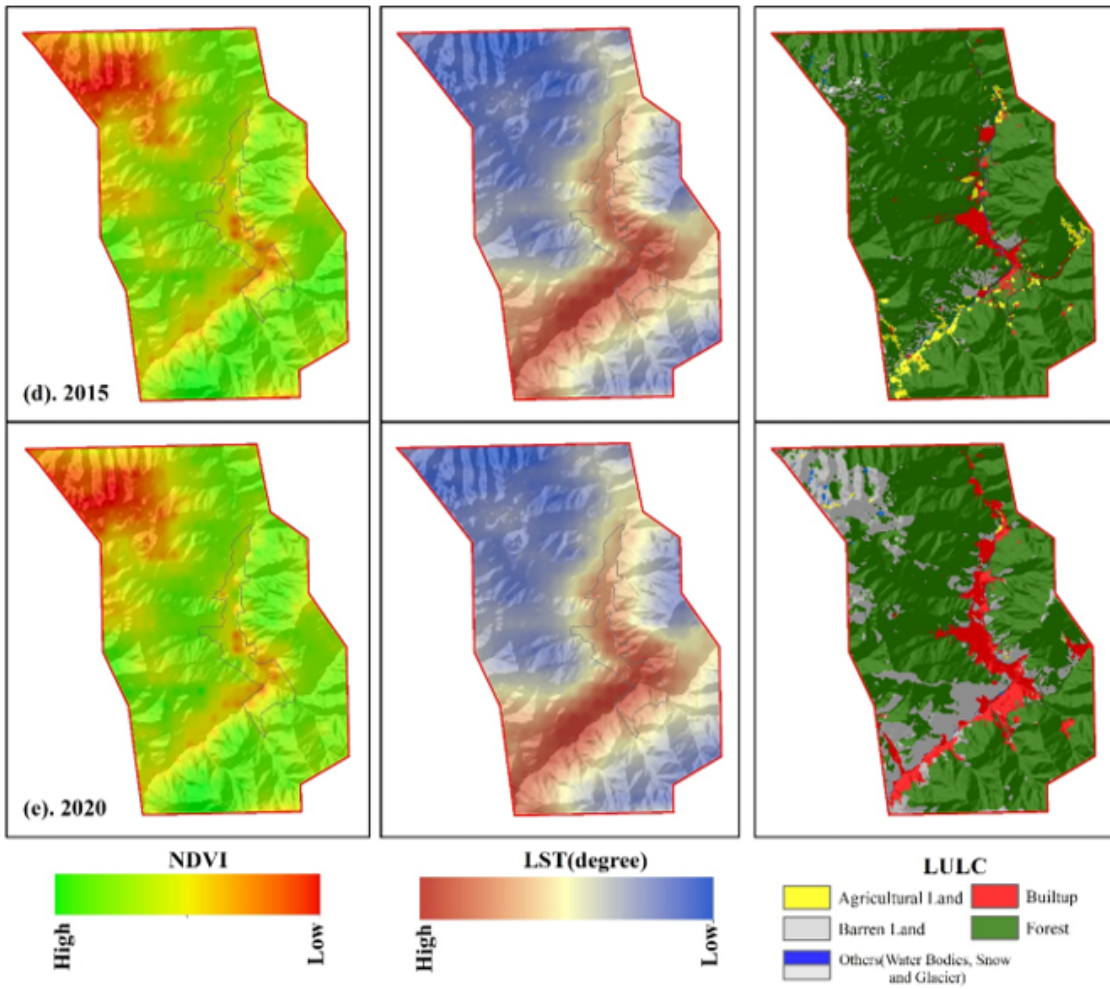
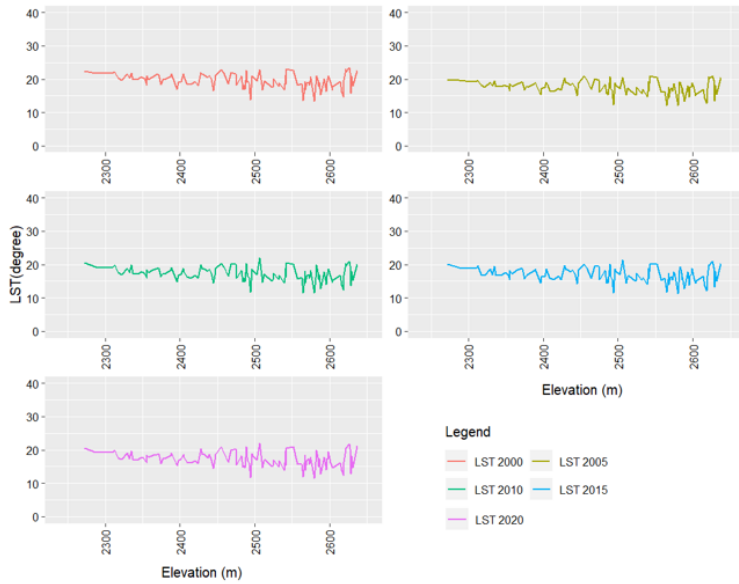
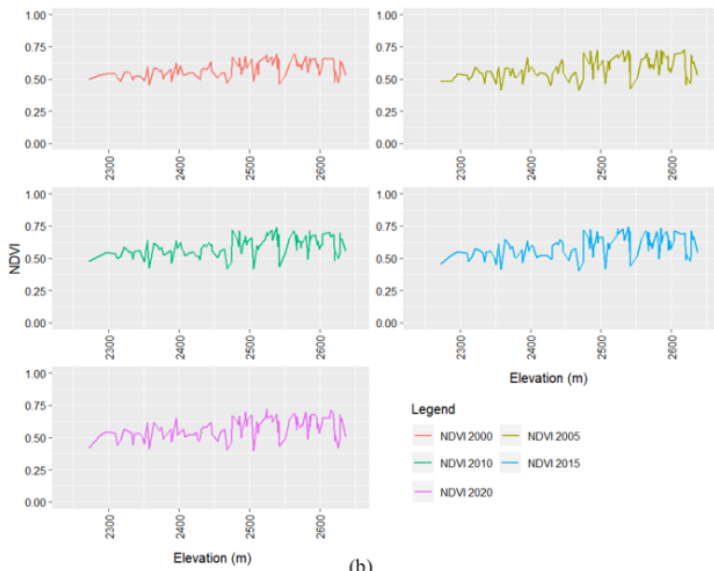


**Figure 6**

Spatial representation of the trend in NDVI, LST, and LULC (d) NDVI, LST, and LULC images of 2015 and (e) NDVI, LST, and LULC images of 2020.



(a)



(b)

## Figure 7

(a): Spatial-temporal analysis of LST vs elevation from 2000 - 2020 at a temporal interval of 5 years.

(b): Spatial-temporal analysis of the NDVI vs elevation from 2000 - 2020 at a temporal interval of 5 years.

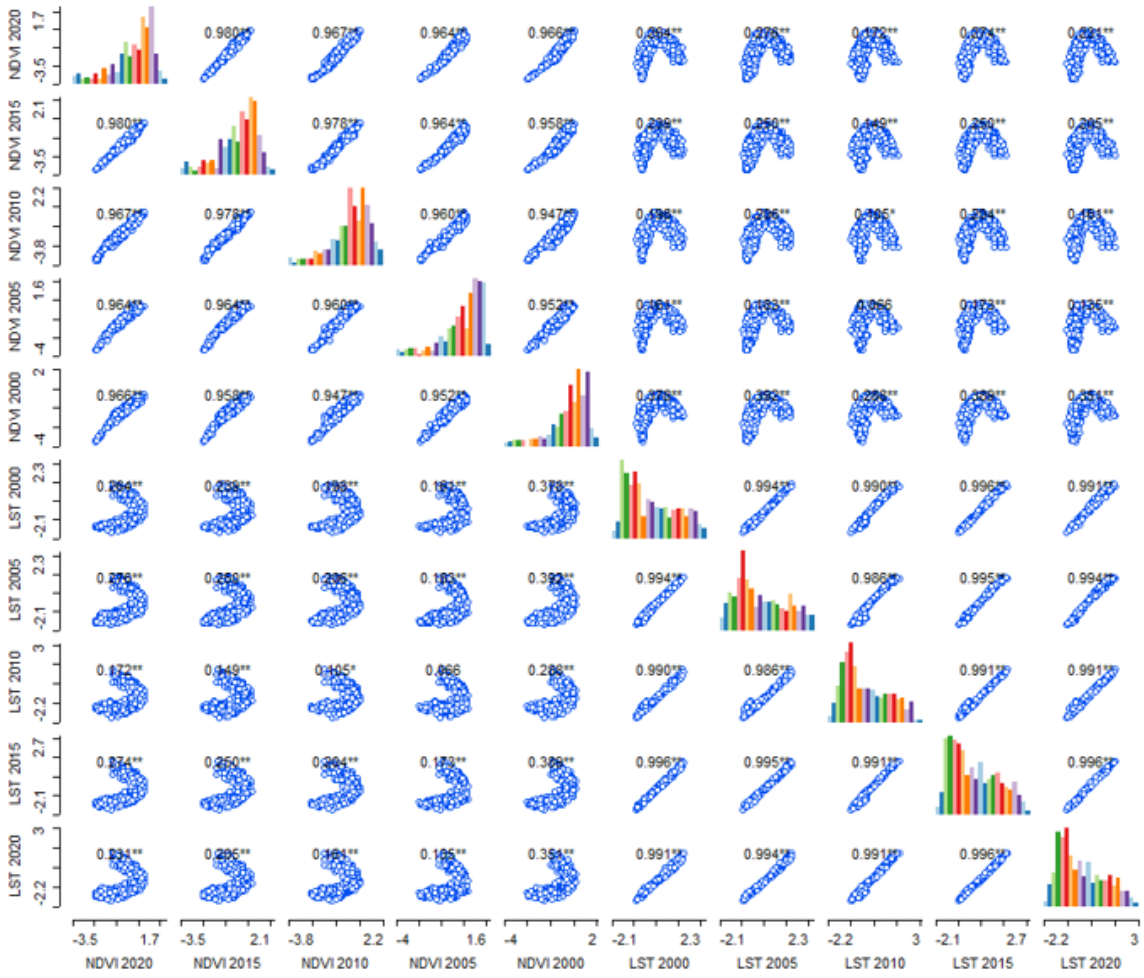


**Figure 8**

Scatter matrix for LST and NDVI for the years between 2000 and 2020. The increasing trend in the LST along with the declining trend in the NDVI across the valley concerning elevation in the region of interest (Figure 1), shows a trend towards increased development activities.

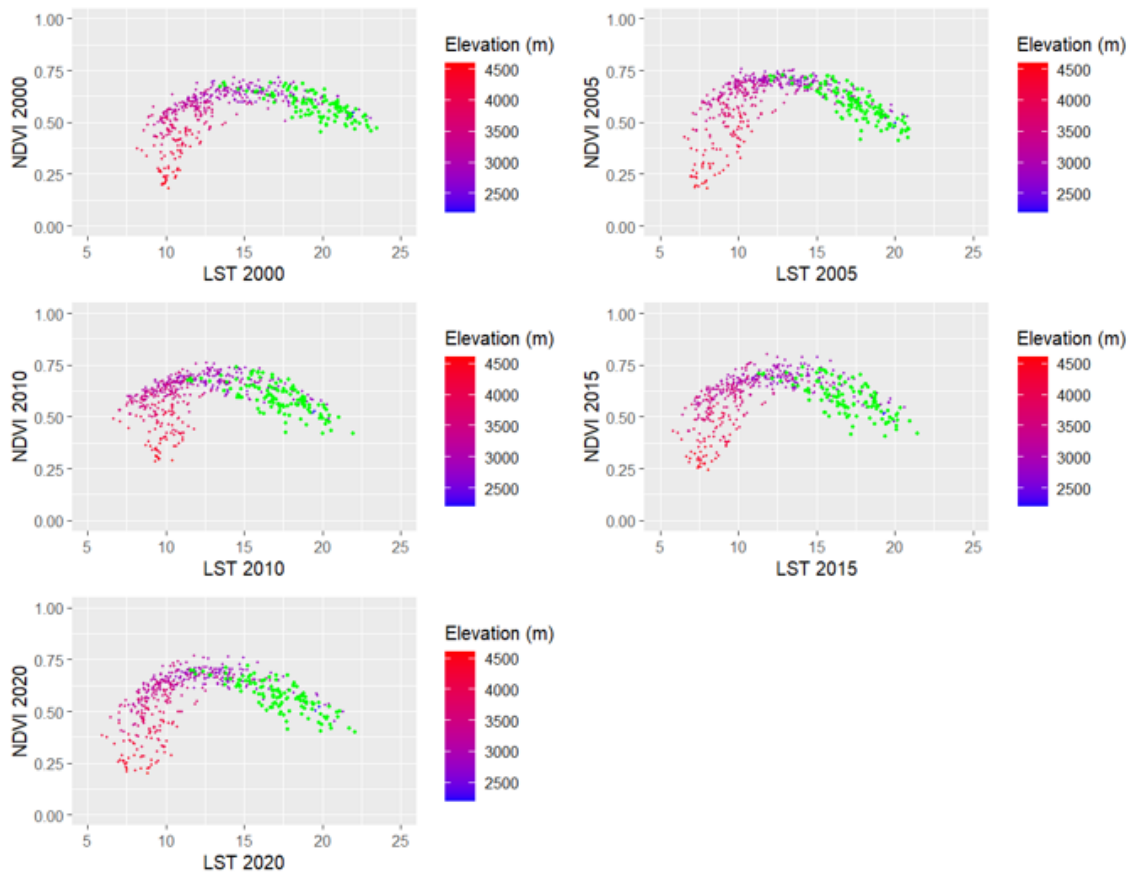


**Figure 9**

Interrelationships between the LST, NDVI, and elevation in 2000, 2005, 2010, 2015, and 2020. The green dots represent the LST and NDVI in the elevation range of Thimphu city.